Article

Model-Assisted Optimization of Cobalt Biosorption on Macroalgae *Padina pavonica* for Wastewater Treatment

Abeer S. Aloufi [1], Bahja Al Riyami [2], Mustafa A. Fawzy [3,4], Hatim M. Al-Yasi [4], Mostafa Koutb [5] and Sedky H. A. Hassan [2,*]

[1] Department of Biology, College of Science, Princess Nourah bint Abdulrahman University, P.O. Box 84428, Riyadh 11671, Saudi Arabia; asaloufi@pnu.edu.sa

[2] Department of Biology, College of Science, Sultan Qaboos University, Muscat 123, Oman; bahja@squ.edu.om

[3] Botany and Microbiology Department, Faculty of Science, Assiut University, Assiut 71516, Egypt; mafawzy@tu.edu.sa or mustafa.fawzy@aun.edu.eg

[4] Biology Department, Faculty of Science, Taif University, P.O. Box 11099, Taif 21944, Saudi Arabia; h.alyasi@tu.edu.sa

[5] Department of Biology, Faculty of Science, Umm Al-Qura University, Makkah 24381, Saudi Arabia; mmkoutb@uqu.edu.sa

* Correspondence: s.hassan@squ.edu.om; Tel.: +968-93879120

Abstract: The release of heavy metals into the environment as a result of industrial and agricultural activities represents one of the century's most significant issues. Cobalt is a hazardous metal that is employed in a variety of industries. In this study, response surface methodology (RSM) combined with Box–Behnken design (BBD) was utilized to optimize the Co(II) ion removal from synthetic wastewater by the brown macroalga *Padina pavonica*. The influence of three factors, namely algal inoculum size, pH, and initial metal concentration, was assessed in optimization studies. RSM proposed a second-order quadratic model with a *p*-value of <0.0001 and R^2 of 0.984 for *P. pavonica*. According to the data related to RSM optimization, the maximum percentage of Co(II) removal of 84.3% was attained under the conditions of algal inoculum size of 5.98 g/L, pH of 6.73, and initial Co(II) concentration of 21.63 mg/L. The experimental data from the biosorption process were fitted well with the Langmuir, Freundlich, and Temkin isotherm models. The maximal Co(II) adsorption capacity was estimated using the Langmuir model to be 17.98 mg/g. Furthermore, the pseudo-second-order kinetic model was shown to have the best fit for Co biosorption by *P. pavonica*, showing that the mechanism of Co(II) biosorption was chemisorption controlled by surface biosorption and intra-particle diffusion. Thermodynamic parameters were also investigated to evaluate the Gibbs free energy for the Co(II) ion, which was positive, showing that the biosorption process is nonspontaneous and exothermic, and the cobalt biosorption rate decreases with increasing temperature. Algal biomass was characterized by Fourier transform infrared spectroscopy, scanning electron microscopy, and energy dispersive spectroscopy. These analyses revealed the biosorbent's diverse functional groups and porous, rough appearance. Therefore, *P. pavonica* can be used to implement sustainable, eco-friendly, and acceptable solutions to water pollution problems.

Keywords: *Padina pavonica*; response surface methodology; optimization; Co(II) ion; biosorption

1. Introduction

Water contamination is one of the most serious environmental issues of the twenty-first century. It is thought to have an impact on food production and the notion of sustainable development [1]. Heavy metals have been a major source of water pollution, and their release into the environment is a severe problem since they are nonbiodegradable, toxic, and have a tendency to accumulate in the food chain [2]. Heavy metals such as cobalt, nickel, cadmium, copper, lead, mercury, and others have significant negative impacts on humans due to their excessive bioaccumulation [3]. However, the extremely high exposure

to cobalt makes it a serious water pollutant that affects not only humans but also other animals and plants [4].

Cobalt-containing compounds are commonly utilized in magnetic alloys, feed additives, pigments, paints, and electroplating, all of which generate considerable amounts of cobalt-containing waste [5]. Exposure of humans to cobalt can cause bone defects, pneumonia, asthma, diarrhea, blood pressure, and paralysis [6]. In plants, however, increased cobalt concentrations can cause necrosis and chlorosis, decrease water and mineral nutrient uptake, and limit root growth [4]. When animals consume higher amounts of cobalt, reproductive abnormalities, neurological difficulties, and heart failure may occur [7]. As a result, cobalt must be removed during wastewater discharge.

Heavy metals have been removed using a variety of physical and chemical removal techniques [8]. Still, biological treatments that use specialized microorganisms are the most cost-effective way to eliminate these pollutants. The adsorption capacity of several microorganisms, such as fungi, yeast, bacteria, micro- and macroalgae, as well as plant byproducts, was examined and showed great potential for the removal of heavy metals from wastewater [9].

Marine brown macroalgae are an attractive group of biosorbents for metal biosorption because they are inexpensive, renewable, have large surface areas, and have the potential for regeneration and metal recovery [10]. The cell walls of brown macroalgae are formed of biopolymers such as alginate and fucoidan, which contribute to their effectiveness. The chemical residues in these biopolymers provide functional groups such as hydroxyl, sulfate, carboxyl, and amino groups that interact with metal ions, resulting in chemical complexation or physical retention, leading to the adsorption of metal ions [11]. Alginate and fucoidan have a stronger affinity for heavy metals, which is represented in the maximal adsorption capacity (q_{max}), where brown macroalgae have greater absorption rates than other forms of algae [12].

Brown macroalgae have been investigated for the removal of many metal ions, such as chromium, gold, uranium, nickel, zinc, cadmium, copper, and lead. The maximum adsorption capacities for all investigated brown algal species and metal ions were high, ranging from 0.39 to 1.66 mmol/g [13,14].

Several factors, including initial metal concentration, pH, temperature, biosorbent concentration, contact time, and static-agitation, can affect the efficacy of heavy metal adsorption [15]. These parameters must be optimized to achieve efficient metal removal, particularly at high concentrations. Enhancing the metal biosorption efficiency by the traditional approaches is costly, time-consuming, and laborious. These drawbacks of the traditional approaches can be overcome by using the response surface methodology (RSM), which decreases the number of tests and facilitates enhancement by examining the impact of individual and reciprocal interactions between factors on the response.

Although considerable efforts have been made in recent decades, additional research is still required to completely investigate the long-term performance and practical applicability of various adsorbents and diverse adsorption methodologies for the removal of various heavy metals.

Therefore, the aim of this work is to optimize independent factors using RSM to maximize cobalt biosorption on the marine brown macroalga *Padina pavonica*. The impact of significant variables such as algal inoculum size, pH, initial cobalt concentration, temperature, and contact time on the biosorption process was investigated. In this study, thermodynamic, equilibrium isotherms, and kinetic models were also studied to evaluate the biosorption mechanism of cobalt ions.

2. Materials and Methods

2.1. Collection of Algae

The brown macroalga *Padina pavonica* (Linnaeus) Thivy was obtained at a depth of 0.3 m in the coastal area of Jeddah (Red Sea), Saudi Arabia. The algae samples were brought to the laboratory, washed with tap water, then deionized water to eliminate salts

and particles, and air-dried at room temperature. Algal biomass was pulverized to powder with an average particle size of 400–600 μm and stored in an airtight bottle.

2.2. Sampling of Agricultural Wastewater

To investigate the efficiency of *P. pavonica* in removing cobalt ions from agricultural wastewater, effluent samples were taken from Wady Al-Arj, Taif, Saudi Arabia, filtered, and stored in the dark at 4 °C.

2.3. Biosorbent Characterization

The analysis of Fourier Transform Infrared (FT-IR) was carried out to characterize the surface functional groups of Co(II) ion-treated and untreated *P. pavonica* biomass. FT-IR spectra were assessed using FT-IR (Bio-Rad, FTS, 3000 MX; Hercules, CA, USA). The morphology and percentage elemental content of *P. pavonica* biomass were investigated using a scanning electron microscope-energy dispersive X-ray spectroscopy (SEM-EDX) (JSM-5400 LV; JEOL; Peabody, MA, USA) at the Unit of Electron Microscope-Assiut University.

2.4. Batch Biosorption Experiments

Batch adsorption experiments were performed to assess the effectiveness of *P. pavonica* in removing Co(II) ions from aqueous solutions. A stock solution of $CoCl_2 \cdot 6H_2O$ (1000 mg/L) was made by dissolving a definite quantity of cobalt chloride in deionized water. Biosorption studies were carried out in 250 mL Erlenmeyer flasks containing 100 mL of Co (II) solution, and the samples were shaken in a rotary shaker (170 rpm) at 25 °C, and the pH was adjusted with 0.1 mol/L of NaOH or HCl.

Three variables, including initial Co(II) concentration, contact time, and temperature, were individually examined in batch adsorption tests to examine their influence on the percentage of Co(II) removal by *P. pavonica*.

The impact of initial Co(II) concentration was investigated at various concentrations of cobalt (20–100 mg/L) under the conditions of algal inoculum size, pH, contact time, and temperature of 6 g/L, 6, 60 h, and 25 °C, respectively.

Additionally, the impacts of varied contact times (0–150 min) were studied at pH 6, algal inoculum size of 6 g/L, initial Co(II) concentration of 40 mg/L, and temperature of 25 °C.

In order to investigate how temperature affects the efficiency of Co(II) removal, experiments were conducted at different temperature values (15–45 °C), and fixed algal inoculum size, pH, contact time, and initial Co(II) concentrations of 6 g/L, 6, 60 h, and 40 mg/L, respectively.

Each experiment was conducted three times and the average data are given. At the end of the biosorption process, the algal biomass was removed from the solution by centrifugation at 5000 rpm for 5 min.

The Buck Scientific 210VGP atomic absorption spectroscopy with flame and graphite furnace atomization techniques (Buck Scientific, Inc., East Norwalk, CT, USA) were used to determine the concentration of Co (II) in the supernatant.

Equation (1) shows the cobalt removal efficiency (Co(II) removal percentage).

$$(\%)\text{Removal} = \frac{(C_i - C_{eq})}{C_i} \times 100 \tag{1}$$

The metal biosorption capacity of the algal biomass (q_e; mg/g) is determined by the following Equation (2):

$$q_e = \frac{(C_i - C_{eq})V}{W} \tag{2}$$

where C_i and C_{eq} are the concentrations of metal ions before and after equilibrium time (mg/L), W is the weight of the biosorbent (g), and V is the volume of the metal solution (mL).

2.5. Experimental Design Using RSM and Statistical Analysis

In this investigation, 17 experiments were performed using a response surface methodology (RSM) based on Box–Behnken experimental design (BBD) with five central point repetitions to investigate the impact of three independent variables at three coded levels (−1, 0, +1) on the percentage of cobalt removal by *P. pavonica*. These variables include algal inoculum size (2–6 g/L), pH (4–8), and initial Co(II) concentration (20–60 mg/L) (Table S1).

The study was carried out at a fixed temperature of 25 °C for 60 min, and the residual concentration of Co(II) was determined following a previously reported method.

Experimental results were analyzed using a second-order quadratic model to determine the linear and quadratic impacts of independent parameters on the removal efficiency of cobalt ions. The polynomial model utilized by the RSM is as follows:

$$Y = \beta_o + \sum \beta_i X_i + \sum \beta_{ii} X_i^2 + \sum \beta_{ij} X_i X_j + \varepsilon \tag{3}$$

where Y is the predicted response, β_o is the intercept term, β_i, β_{ii}, and β_{ij} are the linear, quadratic, and interaction effects, respectively, and X_i and X_j are the independent parameters.

Graphical and regression analyses, as well as ANOVA and experimental design, were performed using Design-Expert software version 7 (Stat-Ease Inc., Minneapolis, MN, USA) to assess interactions between parameters and response (cobalt removal efficiency).

To determine the significance of model terms, the probability value (Prob > F) and Fisher's test (F) were used. The determination coefficient (R^2) was also used to assess the model's reliability.

2.6. Thermodynamic, Isotherm, and Kinetic Studies

After optimization of cobalt removal by RSM, thermodynamic, isothermal, and kinetic analyses were carried out under these optimized conditions.

2.6.1. Thermodynamic Analysis

In the thermodynamic studies, the samples were tested at three different temperatures (293, 303, and 313 K) under the optimum conditions of algal inoculum size of 5.98 g/L, pH of 6.73, and initial Co(II) ion concentration of 21.63 mg/L with an equilibrium time of 60 min. The following equations were used for calculating the thermodynamic parameters:

$$\Delta G^\circ = -RT ln K_C \tag{4}$$

$$Ln K_C = \frac{\Delta S}{R} - \frac{\Delta H}{RT} \tag{5}$$

$$\Delta G^\circ = \Delta H^\circ - T \Delta S^\circ \tag{6}$$

where ΔG°, ΔS°, and ΔH° (kJ/mol) are the Gibbs free energy change, entropy change, and enthalpy change, respectively; R, T, and K_c are the universal gas constant (8.31 J/mol K), temperature (K), and equilibrium thermodynamic constant, respectively.

2.6.2. Isotherm Models

To determine the optimal isotherm models of Langmuir, Freundlich, Temkin, and Dubinin–Radushkevich, a number of experiments were carried out using different concentrations of cobalt (20, 40, 60, 80, and 100 mg/L) under the optimum conditions of algal inoculum size of 5.98 g/L, pH of 6.73, an equilibrium time of 60 min at 25 °C.

The linear Langmuir model is expressed by the following equation:

$$\frac{C_{eq}}{q_e} = \frac{1}{q_{max} K_L} + \frac{C_{eq}}{q_{max}} \tag{7}$$

where q_e represents the amount of Co(II) ion biosorbed on the biosorbent at equilibrium (mg/g); q_{max} represents the maximum sorption capacity (mg/g), and K_L is Langmuir constant (L/mg).

Dimensionless separation factor R_L is evaluated from Equation (8).

$$R_L = \frac{1}{(1 + K_L C_0)} \tag{8}$$

where C_0 is initial Co(II) concentration.

The linear Freundlich model is expressed as follows:

$$Ln\, q_e = Ln\, K_F + \frac{1}{n}\, Ln\, C_{eq} \tag{9}$$

where K_F and n are the adsorption capacity (L/mg) and adsorption affinity, respectively.

The linear Temkin model is represented by the following equation:

$$q_e = Bln A_T + B\, ln C_{eq} \tag{10}$$

$$B = \frac{RT}{b} \tag{11}$$

where A_T is the equilibrium binding constant (L/mg), and b is Temkin isotherm constant related to adsorption heat (J/mol).

The Dubinin–Radushkevich model is determined from the following equations:

$$Lnq_e = lnq_o - \beta\varepsilon^2 \tag{12}$$

$$\varepsilon = RT\, ln\left(1 + \frac{1}{C_{eq}}\right) \tag{13}$$

$$E = \sqrt{1/2\beta} \tag{14}$$

where q_o represents the theoretical saturation capacity of the biosorbent (mg/g), ε and β are the polyani potential and biosorption energy (mol^2/J^2), respectively.

2.6.3. Kinetic Models

Batch studies were also carried out at various contact times (0 to 150 min) and optimal circumstances in terms of algal inoculum size of 5.98 g/L, pH of 6.73, and initial Co(II) concentration of 21.63 mg/L at 25 °C to fit the kinetic models, such as pseudo-first,-second-order, intra-particle diffusion, and Elovich models (Equations (15)–(18)).

The pseudo-first-order model is given by the following equation:

$$Log\,(q_e - q_t) = Log\, q_e - \frac{K_1\, t}{2.303} \tag{15}$$

The pseudo-second-order model is represented by the following equation:

$$\frac{t}{q_t} = \frac{1}{K_2 q_e^2} + \frac{t}{q_e} \tag{16}$$

The intra-particle diffusion model equation is given by the following equation:

$$q_t = K_i t^{1/2} + C_i \tag{17}$$

The Elovich kinetic equation is expressed by the following equation:

$$q_t = \frac{1}{\beta} ln\,(\alpha\beta) + \frac{1}{\beta} ln(t) \tag{18}$$

where q_t (mg/g) is the adsorption capacity at time; k_1, k_2, k_i are the rate constants of pseudo-first-order (min^{-1}), pseudo-second-order (g/mg/min), and intra-particle diffusion equation (mg/g min$^{1/2}$), respectively; C_i is the constant of boundary layer thickness (mg/g); α is the initial rate of biosorption (mg/g min); and β is the constant of desorption (g/mg).

3. Results and Discussion

3.1. Characterization of Biosorbent

The analysis of FT-IR was carried out to identify the functional groups on the surface of the biosorbent involved in cobalt uptake. Figure 1 display the FTIR spectra of treated and untreated *P. pavonica* in the region 4000 cm^{-1} to 400 cm^{-1}.
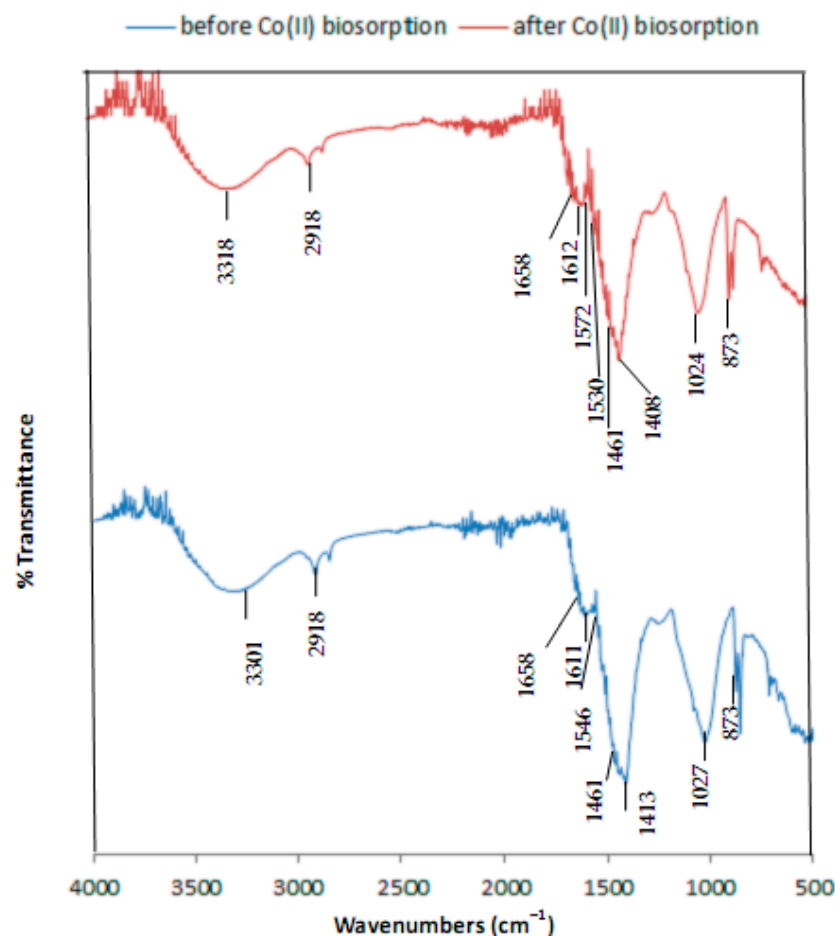

Figure 1. FTIR analysis of *P. pavonica* biomass before and after Co(II) ion biosorption.

In this analysis, several bands associated with the vibrations of the functional groups of the algal biomass were identified. The absorption bands shifting from 3301 cm^{-1} to 3318 cm^{-1} as well as from 1612 cm^{-1} to 1611 cm^{-1} before and after Co(II) biosorption, respectively, are related to anti-symmetric O–H stretching vibrations and the C=O bond found in guluronic and mannuronic acids of alginate [16,17].

The shift in the stretching vibration of –OH showed the formation of hydrogen bonds between the algal biomass and Co ions. The C–H group is represented by the peaks that appeared at 2918 cm^{-1} and 873 cm^{-1}. According to Postai et al. [18], the –C=C– vibrations of the alkene stretch are assigned to the adsorption band of algal biomass at a wavenumber of 1658 cm^{-1}. Furthermore, a carboxylate ion band at 1572 cm^{-1} was detected only on the surface of *P. pavonica* biomass after the biosorption of Co(II) [19].

The presence of an amide group in algal biomass is related to the change in the band from 1546 cm^{-1} (untreated biomass) to 1530 cm^{-1} (treated biomass) [20]. Moreover, the

presence of O–H and C–O stretching frequency was demonstrated by the peak at 1461 cm^{-1}. On the other hand, the shift in the absorption peak from 1413 cm^{-1} to 1408 cm^{-1} is assigned to S=O stretching, confirming the interaction between fucoidan sulfate groups in algal biomass and Co(II) ions via electrostatic attraction [21].

The absorption bands at 1027 cm^{-1} (before biosorption) and 1024 cm^{-1} (after biosorption) can be attributed to the CO group found in esters [18]. It has also been noticed in this analysis that many peaks were appeared in the 1000–500 cm^{-1} range, which could be related to the C–H group.

These findings indicate that cobalt ions bind to the active surface of *P. pavonica* containing different functional groups such as carbonates and sulfates via electrostatic attraction between these groups and Co(II) ions. The interaction of Co(II) ions with the active sites of *P. pavonica* resulted in a shift in the wavenumber of the functional groups, variations in the absorption strength, and the formation of new absorption peaks. The current study revealed that carboxyl, sulfate, hydroxyl, carbonyl, amide, and carbonate play important roles in cobalt uptake by *P. pavonica*.

SEM analysis was also used to clarify the differences in the treated and untreated surfaces of *P. pavonica* biomass (Figure 2A,B). Untreated algal cells displayed a rough, irregular, and porous surface with variable shapes and sizes (Figure 2A). These features facilitate rapid mass penetration during the biosorption of cobalt on the surface of *P. pavonica* and allow greater interaction of Co(II) ions with the algal structure [22].
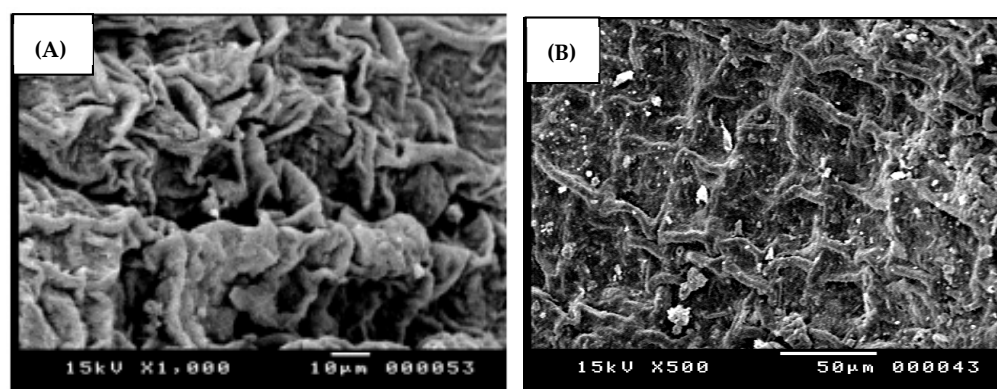

Figure 2. Analyzed SEM micrograph of (**A**) untreated and (**B**) treated *P. pavonica* biomass with Co(II) ions.

After being exposed to Co(II) ions, the *P. pavonica* surface changed, and reduced pores were observed (Figure 2B). This observation implies that Co(II) ions accumulate on the surface of the algal cells and bind to their functional groups. Additionally, metal ions may create stronger linkages by substituting the cations that are already present in the cell wall matrix. The metal ion may occupy available binding sites based on ion exchange theory [23].

The EDX data revealed that the structure of algal biomass contains small quantities of phosphorus and sulfur, as well as a number of alkaline ions, including calcium, sodium, magnesium, aluminum, and silicon.

An ion exchange mechanism, in which the algal biomass's acidic functional groups exchange protons and/or cations of alkali metals with Co(II) ions, may be responsible for the biosorption of Co(II) by the algal biomass (Figure 3) [24].

The EDX analysis also revealed that the bands present only after cobalt biosorption from 6.8 to 7.2 keV (Figure 3B) display cobalt binding energies, with a cobalt percentage of 5.23% and consequently, the EDX analysis confirmed Co(II) biosorption by *P. pavonica* [25].
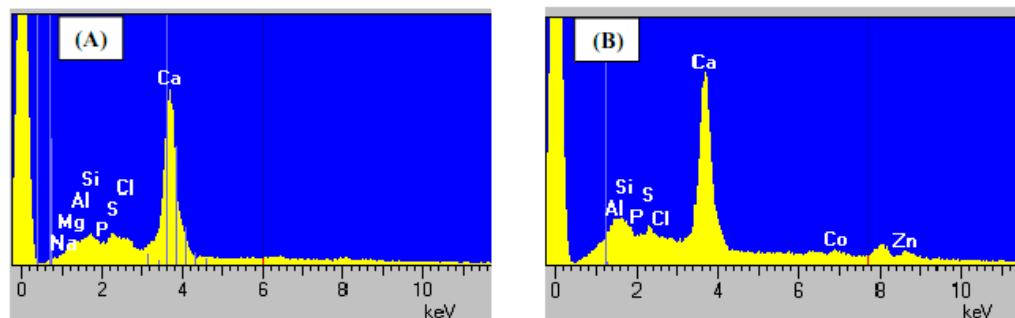
Figure 3. Elemental distribution by EDX analysis of (**A**) untreated and (**B**) treated *P. pavonica* biomass with Co(II) ions.

3.2. Biosorption Parameter Study

The Impact of Initial Co(II) Concentration, Contact Time, and Temperature on the Removal Efficiency of Co(II) Ions

The influence of initial Co(II) ion concentrations (20, 40, 60, 80, and 100 mg/L) on the cobalt removal efficiency of *P. pavonica* was investigated at a fixed pH value of 6.0, a contact time of 60 h, an algal inoculum size of 6 g/L, and a temperature of 25 °C.

According to the data depicted in Figure 4A, when the concentration of Co(II) ion increases from 20 to 100 mg/L, the efficiency removal of Co significantly decreases from 88.15% to 73.96% ($p < 0.05$). A higher cobalt removal percentage was observed at low Co(II) concentrations due to the many freely available sites on the surface of algal biomass [26]. Additionally, it is probable that Co(II) ions preferentially diffuse through the active sites of *P. pavonica* biomass at lower cobalt concentrations.
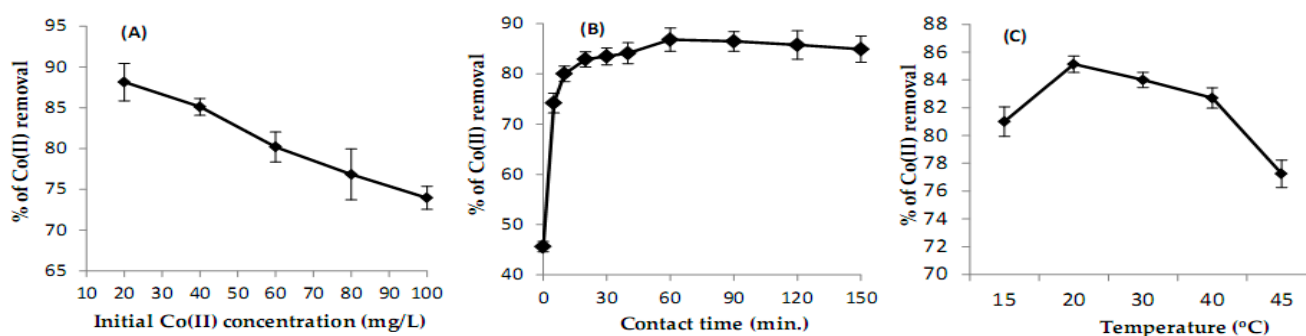

Figure 4. Effect of initial Co(II) concentration (**A**), contact time (**B**), and temperature (**C**) on the percentage of Co^{2+} removal by *P. pavonica*. Each data point shows the average $\pm$ SE.

The decrease in cobalt uptake by *P. pavonica* is caused by an excessive number of cobalt ions that outnumber the available adsorption sites [27].

Contact time is another significant parameter that influences the adsorption process by estimating the equilibrium time, which is defined as the time needed for heavy metals in an aqueous solution to reach a constant value (i.e., maximum adsorption).

Figure 4B indicates the impact of different contact times (0–150 min) on the biosorption of Co(II) ions on *P. pavonica*. The removal efficiency increased significantly ($p < 0.05$) within the first 20 min and achieved adsorption equilibrium (86.83%) within 60 min. After that, the cobalt removal became extremely slow. The fast alteration in the percentage of cobalt removal within 20 min may be due to more binding sites on the algal surface [28]. However, as these sites are increasingly occupied, the adsorption efficacy decreases, which slows down the biosorption process. Over time, it gets harder to occupy the remaining available sites on the biosorbent as a result of the formation of repulsive interactions between the metal ions on the surface of the biosorbent and the solution, which brings the system to equilibrium [29].

According to Li et al. [30], during the adsorption process, the number of active sites is limited, and the existence of metal ion competition reduces the metal uptake until the equilibrium time is reached. Accordingly, Bai and Venkateswarlu [31] pointed out that metal ions form a single-molecule-thick layer on the biosorbent surface, and the sorption process slows down over time.

The impact of temperature (15–45 °C) on cobalt removal percentage by *P. pavonica* was studied at fixed circumstances of pH 6.0, equilibrium time of 60 h, 6 g/L algal inoculum size, and 40 g/L initial metal concentration. Temperature has a negative impact on the percentage of cobalt removal.

The highest removal rate of Co(II) ions (more than 85%) was recorded at a low temperature (20 °C; Figure 4C). On the other hand, the adsorption efficiency of Co ions by *P. pavonica* was reduced by a rising temperature (45 °C). These results are consistent with the findings of Ranaweera et al. [29], who reported that the cobalt removal efficiency of cleaning nut seed powder (*Strychnos potatorum*) decreased with increasing temperature. The results of the current study showed that biosorption activity is partially deactivated at temperatures above 20 °C. This may be related to the tendency of heavy metals to escape when the solution temperature increases from the solid phase to the bulk [32]. As a result, the mechanism of the biosorption process could involve electrostatic interaction, which is commonly related to adsorption at low temperatures. This conclusion was verified by FTIR analysis, which showed the existence of absorption peaks related to the sulfate groups of fucoidan in algal biomass, indicating that these groups interact with Co(II) ions through electrostatic attraction.

3.3. Box–Behnken Design (BBD) and Data Analysis

3.3.1. Model Development

The influences of algal inoculum size, pH, and initial cobalt concentration on the adsorption process were examined and optimized using response surface methodology (RSM) with Box–Behnken experimental design (BBD). Table S1 displays the experimental design and expected and actual biosorption data.

The removal efficiency of cobalt ranged from 68.70% at an algal inoculum size of 2 g/L, pH value of 6, and an initial cobalt concentration of 60 mg/L (Std. order 7) to 87.95% at an algal inoculum size of 6 g/L, pH 6, and initial cobalt concentration of 20 mg/L (Std. order 6) (Table S1). In addition, the actual results for Co(II) uptake by *P. pavonica* biomass were close to the predicted data from BBD.

The optimal biosorption efficiency was determined using a second-order polynomial equation based on BBD. According to the obtained data, a quadratic equation (Equation (4)) was developed to relate the Co(II) removal efficiency to the independent input variables of the coding terms in the quadratic model, and nonsignificant variables were removed using a backward process.

The negative and positive signs associated with the regression coefficients in this equation indicate the nature of the modeling terms' influence on the adsorption efficiency of algal biomass:

$$\% \text{ removal (Co(II) ion)} = 79.95 + 5.65A + 1.10B - 4.61C - 1.26AB - 1.18A^2 \quad (19)$$

where A, B, and C are the coded levels of the independent parameters—algal inoculum size (g/L), pH, and initial Co(II) concentration (mg/L), respectively.

3.3.2. ANOVA Analysis

The ANOVA results are used to assess model performance and interactions between different factors and responses [33]. A significant model in ANOVA was verified with a *p*-value, indicating the model's enhanced significance [34]. The terms of the quadratic model are significant if the *p*-value (prob. > F) is below 0.05 and vice versa [35].

In this investigation, the *p*-value of the model was less than 0.0001, showing that the model was accurate (Table 1). Furthermore, the model *F*-value of 99.89 and the insignificant

value of the lack of fit ($p = 0.0941$) suggested the significance of the polynomial quadratic model [36].

Table 1. ANOVA and significance test for the RSM polynomial quadratic model.

Source	CE	SS	df	MS	*F*-Value	*p*-Value Prob > *F*
Model	-	446.05	9	49.71	99.89	<0.0001 *
A-algal dose	5.65	255.38	1	255.38	285.94	<0.0001 *
B-pH	1.10	9.75	1	9.75	10.92	0.011 *
C-Co(II) conc.	−4.61	169.74	1	169.74	190.05	<0.0001 *
AB	−1.26	6.38	1	6.38	7.14	0.02 *
AC	0.15	0.09	1	0.09	0.06	0.814 **
BC	0.29	0.35	1	0.35	0.244	0.647 **
A^2	−1.18	5.1	1	5.1	5.38	0.043 *
B^2	0.05	0.008	1	0.008	0.005	0.944 **
C^2	−0.53	0.882	1	0.882	0.614	0.477 **
Residual		5.74	4	1.435		
Lack of Fit		5.73	3	1.909	66.52	0.0941 **
Pure Error		0.02	1	0.02		
Cor. Total		453.20	13			
R^2				0.984		
R^2-adjusted				0.974		
R^2-predicted				0.948		
% C.V.				1.19		
Adequate precision				33.16		

Notes: SS: sum of squares; CE: coefficient estimate; df: degree of freedom; C.V.: coefficient of variation; and MS: mean square. * Significant at $p < 0.05$; ** not significant at $p > 0.05$.

Other descriptive data were also used to evaluate the accuracy of the model, as indicated in Table 1. To assess how well the model approximates the actual results, the determination coefficient (R^2) was used. The goodness-of-fit statistics for this study yielded a reasonable R^2 value of 0.984, suggesting that the quadratic model can explain about 98.4% of the variation in cobalt uptake. Furthermore, the adjusted R^2 value of 0.974 was near the expected R^2 value (0.948), indicating that the model is adequate and dependable.

The value of the variation coefficient (C.V) was 1.19%, indicating that the model is highly replicable and consistent with small differences between experimental and expected data [37]. The adequate precision for determining the ratio of signal-to-noise is 33.16. A virtuous ratio greater than four implies that the model's noise-to-ratio is placed on the appropriate board and that the model may be used to navigate the design space [36].

3.3.3. Response Surface Analysis and the Optimization of Co(II) Biosorption

To enhance the adsorption efficiency of Co(II) ions by *P. pavonica*, the biosorption process needs to be optimized by determining the optimal combination of independent variables to maximize cobalt uptake by algal biomass, followed by model validation.

Figure 5A–C demonstrate 3D plots of the effects of algal inoculum size, pH value, and initial Co(II) concentration on cobalt ion removal efficiency. The 3D curves show the interaction of these parameters and the maximum removal efficiency.

Figure 5A shows the 3D chart of the Co(II) removal percentage of *P. pavonica* under the simultaneous effect of algal inoculum size and pH value. The detected effects of the two evaluated factors on biosorption efficiency were similar, and increasing both parameters significantly enhanced the percentage of cobalt removed by *P. pavonica*.

The highest Co removal rate was observed when the algal inoculum size was 6 g/L and the pH was 8. ANOVA data confirmed these findings and showed that changes in algal inoculum size and pH had linear, positive, significant impacts ($p < 0.01$; Table 1). In other words, as the pH value and biosorbent dosage increase, the removal efficiency of Co ions also increases.
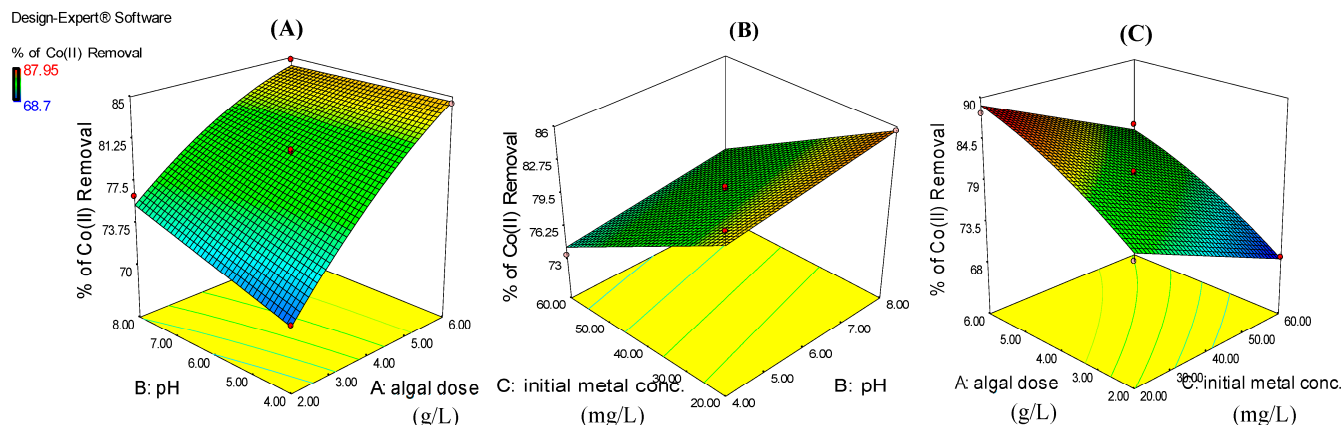
Figure 5. (**A**–**C**). Three-dimensional charts assessing the impact of the combinations of the independent parameters on the percentage of Co(II) removal.

The inoculum size of the biosorbent is one crucial factor that might impact both the adsorption process's efficiency and its performance [38].

When the algal dosage increased from 2 g/L to 6 g/L, the percentage of Co removal increased from 71% to 84%. This is due to the increase in biosorbent surface area and the availability of additional binding sites on the algal biomass surface [39]. Most studies display that raising biosorbent dosage creates more adsorption sites for metal ions to bind. In other words, the possibility of the adsorbent interacting with the metal ions increases, thereby increasing the cobalt removal efficiency [40].

The pH value of the solution can directly regulate the reaction by altering the charges of metal ions and adsorbents and is one of the important factors influencing adsorption efficiency [38].

A reduction in pH resulted in a decrease in the percentage of Co(II) removed by the algal biomass. This is due to the formation of additional positively charged hydrogen ions in aqueous solutions under acidic conditions, and the active binding sites on the algal surface bind tightly to these hydrogen ions, making them unable to bind to other cations [41]; this may be the reason for the low removal efficiency at pH 4. Furthermore, Kumar and Kirthika [42] proposed that at low pH values, more positively charged hydrogen ions surround the biosorbent surface, thereby decreasing the interaction of adsorbate with the biosorption sites of biosorbent due to electrostatic repulsion between the metal ions and the biosorbent, leading to reduced biosorption efficiency.

However, when the pH rises (pH = 8), the algal surface becomes negatively charged and deprotonated, thus enhancing the biosorption process and consequently increasing the percentage of cobalt removal [43]. This is due to the fact that Co(II) ions are positively charged in aqueous solutions; therefore, cobalt biosorption is more efficient when the charge of the algal surface is negative [44]. Soleymani et al. [45] reported similar results regarding Co(II) uptake and found that *Sargassum* sp. had the highest biosorption capacity at pH 7.0.

Figure 5B depicts the interactive effect of pH and initial metal concentration on the percentage of Co(II) removal by *P. pavonica*.

One of the main factors influencing the ability to resist metal ion mass transfer between the adsorbent and the solution is the initial concentration of metal ions [46]. The initial cobalt concentration axis in the 3D plot has a smoother curve and a lower linear coefficient estimate (−4.61; Table 1), indicating that its second-order polynomial term has a higher effect than pH.

Although pH and initial metal concentration had significant effects on removal efficiency, ANOVA findings showed that initial Co(II) concentrations had a greater impact ($p < 0.0001$) on the efficiency of cobalt biosorption than pH ($p = 0.011$).

The highest Co elimination was found at pH 8 and an initial adsorbate concentration of 20 mg/L, as shown in Figure 5B. For instance, the percentage of Co biosorption onto algal biomass was 74.25% at pH 4 and an initial cobalt concentration of 60 mg/L, which increased to 86% at pH 8 and an initial cobalt concentration of 20 mg/L. Cobalt uptake decreases with increasing Co ion concentration because biosorbed Co(II) ions saturate the biosorption sites, resulting in negligible biosorption [47].

The 3D chart in Figure 5C shows the effect of biosorbent dosage and initial adsorbate concentration on the Co(II) removal percentage. These figures display that raising the algal inoculum size and decreasing the initial Co concentration increased the efficiency of Co(II) removal by *P. pavonica*. The findings of the ANOVA confirmed this and demonstrated that the biosorbent dosage and metal concentration had significant effects ($p < 0.0001$; Table 1).

The synergistic removal efficiency was highest (approximately 88%) when the algal inoculum size was 6 g/L and the initial Co concentration was 20 mg/L. This means that increasing the biosorbent dosage while decreasing the initial cobalt concentration can achieve the highest removal efficiency.

3.3.4. Validation and Confirmation of the Quadratic Model

After determining the model's statistical significance, the experimental results were validated to confirm the validity and precision of the model.

The objective of the optimization process was to maximize the rate of Co(II) removal by optimizing the independent variables of Co(II) ion removal. The experiments were carried out in triplicate so that the findings obtained under ideal conditions could be compared with the simulated values of the quadratic model.

Under the optimal conditions of algal inoculum size 5.98 g/L, pH 6.73, and initial Co(II) ion concentration 21.63 mg/L, the optimal removal efficiency was 84.3%, which is consistent with the expected value of 88.55% and confirmed the accuracy and predictability of the proposed model.

3.4. Thermodynamic Properties

A thermodynamic study of Co (II) ion biosorption by algal biomass was carried out at various temperatures (293, 303, and 313 K) using the optimized conditions of BBD (algal inoculum size of 5.98 g/L, pH of 6.73, and initial Co(II) ion concentration of 21.63 mg/L) and contact time of 60 min.

To assess whether the biosorption of cobalt ions on *P. pavonica* occurs spontaneously, the parameters of thermodynamic analysis such as Gibbs free energy change (ΔG°), entropy change (ΔS°), and enthalpy change (ΔH°) were used (Table 2). The aforementioned parameters suggest that the biosorption process may take place at different temperatures [48].

Table 2. Thermodynamic parameters calculated for Co(II) ion biosorption on *P. pavonica* biomass.

Temperature (K)	ΔG°	ΔH°	ΔS°	R^2
	(kJ/mol)			
293	0.115			
303	0.336	−6.84	−0.024	0.998
313	0.590			

The positive charge of the ΔG° value indicates that the biosorption process is not spontaneous, as shown in Figure 6 and Table 2. Furthermore, the value of ΔG° increased with increasing temperature, demonstrating that the biosorption of Co(II) ions on *P. pavonica* biomass was favored with reducing temperature (Table 2).
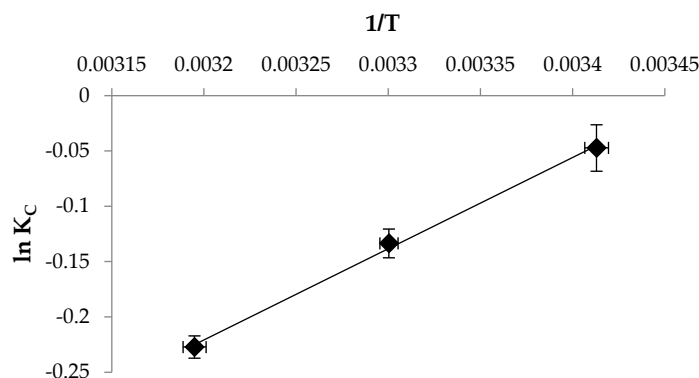
1/T

Figure 6. The plot of lnK_c against $1/T$ for the assessment of the thermodynamic parameters for the Co ion biosorption on *P. pavonica*. Each data point shows the average ± SE.

The fact that ΔH^o is negative suggests that the biosorption process is exothermic. As a result, Co removal effectiveness increases as the temperature decreases [49]. Raising temperature makes the functional groups on the surface of algal biomass more mobile, leading to the detachment of biosorbed Co(II) ions from the algal surface and a subsequent decrease in adsorption rate.

Moreover, the negative value of ΔS^o (-0.024 kJ/mol) indicates a slight increase in the regularity at the liquid–solid interface due to the biosorption of Co(II) ions on the *P. pavonica* biomass [50].

3.5. Isotherm Model for Biosorption

The results of the Co(II) biosorption study were fitted to the Langmuir, Freundlich, Temkin, and Dubinin–Radushkevich (D–R) isotherm models and these models were evaluated under optimal circumstances provided by BBD. Figure 7 and Table 3 show the linear plots, equations, and parameters of isotherm models.

The Langmuir isotherm model better describes the experimental data of Co(II) ion biosorption on algal biomass, which is verified by the high value of determination coefficient ($R^2 = 0.984$; Figure 7A, Table 3), confirming that the biosorption process occurred in a monolayer manner. It indicates that the biosorption rate of cobalt is relatively high [51]. Langmuir linearization confirmed that *P. pavonica* biomass had a maximum biosorption capacity ($q_{max} = 17.98$ mg/g).

Furthermore, the affinity of cobalt ions to the biosorption sites on the surface of *P. pavonica* biomass was high ($K_L = 0.075$ L/mg; Table 3), indicating its good ability to remove Co(II) ions from aqueous solutions. This may be attributed to the fact that the alginate found in the cell wall of brown algae facilitates the biosorption of metals by *P. pavonica* because the functional carboxyl groups in the mannuronic and guluronic acids of the alginate act as active biosorption sites for metals, as verified by FT–IR data. In this regard, Khani [52] stated that the Langmuir isotherm provided an explanation of the ion exchange mechanism for the biosorption process.

Deviations from the linearity of biosorption are taken into account when determining the second parameter (dimensionless factor; R_L) of the Langmuir isotherm model. The R_L value is between zero and one, showing favorable biosorption. Its value ranges from 0.104 to 0.284 (Table 3), indicating that *P. pavonica* and Co(II) ions have good biosorption.

The Freundlich model was evaluated using two parameters: adsorption capacity (K_F) and adsorption intensity (n). The K_F value of algal biomass in this investigation was 1.85 L/mg, showing that algal biomass has a high biosorption capacity for Co(II) (Table 3; Figure 7B). This finding is consistent with previous research [53].

The high biosorption intensity of algal biomass in the current study ($n = 1.69$) reveals that *P. pavonica* biomass favorably biosorbs Co(II) ions and produces considerably stronger bonds with *P. pavonica* biomass, indicating a chemisorption process [54]. Therefore, the

biosorption of Co(II) ions on *P. pavonica* biomass may continue by multilayer biosorption on top of the already chemisorbed layer.
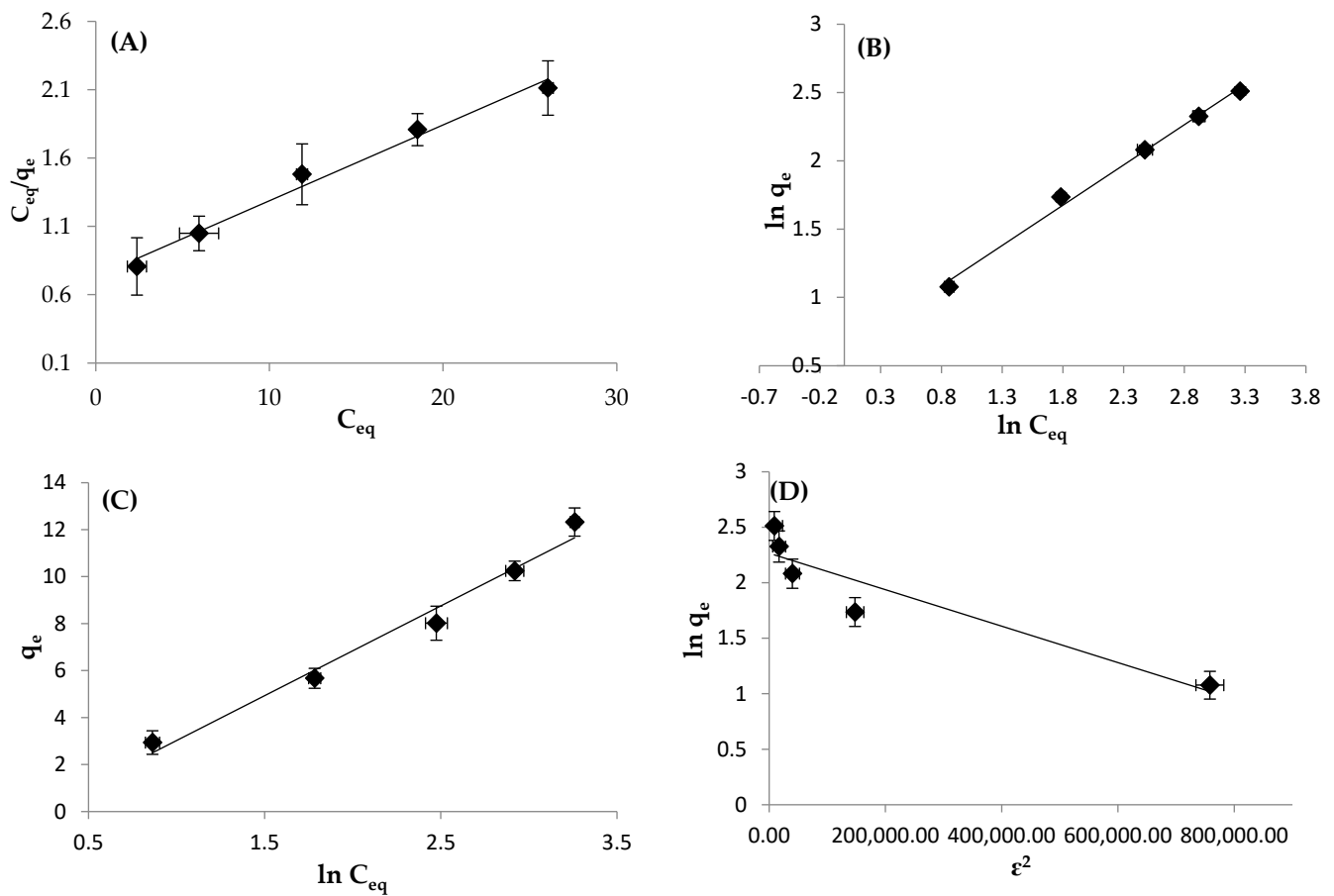

Figure 7. Different isotherm models of cobalt ion biosorption. (**A**) Langmuir, (**B**) Freundlich, (**C**) Temkin, and (**D**) Dubinin–Radushkevich. Each data point shows the average $\pm$ SE.

Table 3. Isotherm parameters calculated for Co(II) ion biosorption on *P. pavonica* biomass.

Models	Parameters	Values
Langmuir	q_{max} (mg/g)	17.98
	K_L (L/mg)	0.075
	R_L	0.104–0.284
	R^2	0.984
Freundlich	n	1.69
	K_F (L/mg)	1.85
	R^2	0.994
Temkin	A_T (L/mg)	1.23
	b (J/mol)	648.6
	R^2	0.978
D–R	q_o (mg/g)	9.64
	$\beta \times 10^{-6}$ (mol^2/J^2)	2.00
	E (kJ/mol)	5.00
	R^2	0.863

In this regard, Sahu et al. [55] reported that the greater the n value, the more powerful the reaction between the adsorbate and the biosorbent. Furthermore, the higher R^2 value (0.994) suggests that multilayer biosorption plays a role in the process mechanism. It

also demonstrates that the Freundlich isotherm model precisely reflects the biosorption equilibrium of Co(II) by algal biomass within the studied concentration range, with high affinity between the heterogeneous algal surface and Co(II) ions [56].

The Temkin isotherm model also confirmed the possibility of heterogeneous sites with different binding energies in good agreement with experimental results [57]. Based on the results in Table 3, the Temkin model was found to be suitable for the biosorption of Co(II) ions on *P. pavonica* biomass, as presented by the high R^2 value (0.978; Figure 7C). These findings provide additional evidence to support the results that chemisorption may be involved in the Co(II) biosorption process.

The higher b value (648.6 J/mol) indicates a strong ion exchange mechanism and the interaction between the Co(II) ions and various functional groups on the algal surface, which is related to the reduction in the adsorption heat of ions in the layer [58]. These results were supported by the characterization of the algal biomass.

The Dubinin–Radushkevich (D–R) isotherm model (Figure 7D) can be used to evaluate whether the adsorption process is a physical (E < 8 kJ/mol) or chemical (E > 16 kJ/mol) adsorption process. The average biosorption energy (E, kJ/mol) is related to the energy of metal ion transport to the surface of the biosorbent.

In this study, the mean free energy (E) of *P. pavonica* was less than 8 kJ/mol (5 kJ/mol), demonstrating that the biosorption process of Co ions is physical adsorption [33].

From the above data, it can be noticed that the R^2 values of Langmuir, Freundlich, and Temkin biosorption isotherms are all greater than 0.97, indicating that the biosorption process is multi-mechanistic and most likely proceeded with a multilayer physisorption on top of the already chemisorbed layer. The biosorption mechanism can be explained by the functional groups present in the algal biomass that assisted in the electrostatic interaction between Co(II) ions and the algal surface.

Table S2 compares the maximum sorption capacity of different materials for Co(II) ions. It can be seen that the ability of *P. pavonica* biomass to remove Co(II) ions is higher than the Co(II) sorption capacity of some adsorbents reported in the literature [1,20,31,59–66]. The variations in the adsorption capacity of Co ions among the adsorbents may be due to differences in the morphological and physico-chemical properties of the adsorbents, including the nature of the adsorbent, particle size, specific surface area, and adsorption conditions investigated [67]. As a result, the availability of *P. pavonica* could provide a cost-effective biosorbent source for heavy metal sequestration from wastewater.

3.6. Kinetic Model for Biosorption

Kinetic plots were modeled using the kinetic models described in Table 4 to assess if Co(II) ion biosorption occurs via chemical interactions with the functional groups of biosorbent or merely by diffusion through the particles of the biosorbent.

Figure 8 depicts linear plots of kinetic models, which include pseudo-first-order, pseudo-second-order, intra-particle diffusion, and Elovich models. The prefix "pseudo" may indicate that an adsorption rate law is expressed in terms of occupied adsorption sites or adsorption quantity "qe" instead of in terms of the concentration of adsorbed metals "C" [68].

Table 4 shows the parameters of the pseudo-first-order kinetic model, revealing that the experimental maximum biosorption capacity of *P. pavonica* (q_{max} = 5.788 mg/g) was considerably higher than the predicted data (q_e = 1.328 mg/g). Furthermore, the low R^2 value (0.788) suggested that the pseudo-first-order kinetic model was not suitable for the biosorption of Co(II) on *P. pavonica* biomass (Figure 8A).

On the other hand, the R^2 value of the pseudo-second-order kinetic model was greater than 0.99; moreover, the expected q_e (5.794 mg/g) was very close to the experimental q_{max} (5.788 mg/g) (Table 4; Figure 8B). These results suggest that Co(II) ion biosorption on algal biomass depends on chemical adsorption, including electron exchange between Co(II) ions and algal biomass, as covalent forces and ion exchange, where Co(II) ions are bound to the surface of algal biomass by chemical bonding [69]. As shown in FT-IR data,

the binding sites on the *P. pavonica* biomass surface include abundant groups like hydroxyl and carboxyl, providing a good possibility for chemisorption.

Table 4. Kinetic parameters calculated for the biosorption of Co(II) ions on *P. pavonica* biomass.

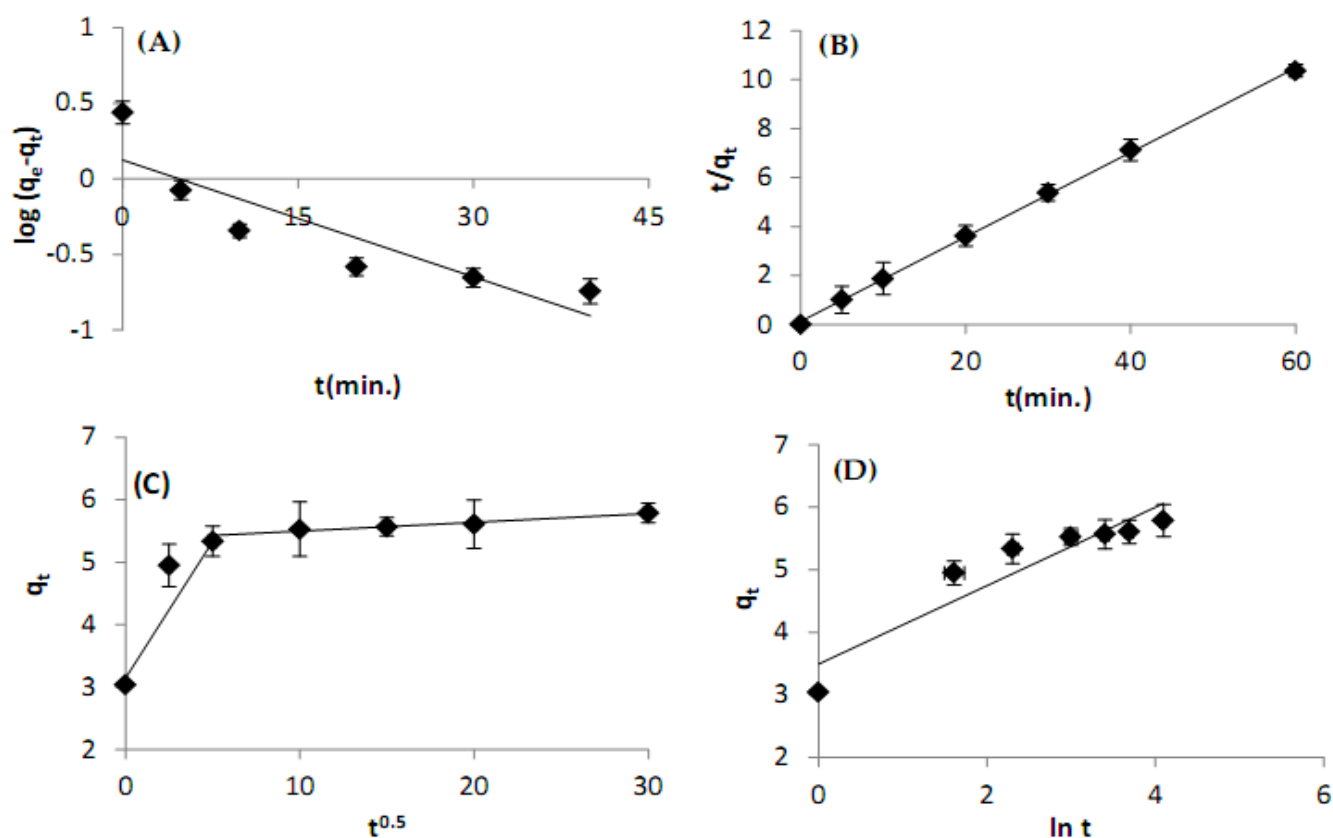| Models	Parameters	Values
Experimental data	q_{max} (mg/g)	5.788
Pseudo-first-order	q_e (mg/g) k_1 (min^{-1}) R^2	1.328 0.059 0.788
Pseudo-second-order	q_e (mg/g) k_2 (g/mg/min) R^2	5.794 0.23 0.999
Intra-particle diffusion	K_{i1} (mg/g min$^{1/2}$) K_{i2} (mg/g min$^{1/2}$) C_{i1} (mg/g) C_{i2} (mg/g) R^2_1 R^2_2	0.459 0.016 3.295 5.303 0.872 0.935
Elovich	α (mg/g min) β (g/mg) R^2	1.81×10^5 1.593 0.871

Figure 8. Different kinetic models of cobalt ion biosorption. (**A**) Pseudo-first-order, (**B**) pseudo-second-order, (**C**) intra-particle diffusion, and (**D**) Elovich. Each data point shows the average ± SE.

As a result, the pseudo-second-order model proved the best fit for characterizing the Co(II) ion biosorption on *P. pavonica* biomass. However, the Dubinin–Radushkevich model suggests that this system has a physisorption mechanism. Consequently, the biosorption

of cobalt on algal biomass may only be thought of as chemical adsorption enhanced by physical processes in nature.

The pseudo-second-order model for *P. pavonica* is the same kinetic model that determines the biosorption kinetics of Co(II) ions for some biosorbents, including *Sargassum* sp. [45], biochar of *Scenedesmus dimorphus* [70], *Ulva fasciata* and *Colpomenia sinuosa* [20], or oxidized activated carbons [15].

The intra-particle diffusion model was also found to fit the plot of qt against $t^{0.5}$ (Figure 8C). Linear plots of this model do not pass through the origin, and the plots consist of two parts. The first region represents quick Co(II) biosorption on the biosorbent's outer surface, while the second region represents equilibrium uptake. This indicates that the intra-particle diffusion step is involved in Co(II) biosorption on algal biomass but not in rate control [71]. This suggests that the biosorption of cobalt ions may have a complex mechanism involving surface biosorption and intra-particle diffusion [72].

The Elovich kinetic model proposes heterogeneous active biosorbent sites with different sorption energies [50]. The data in Table 4 show a low determination coefficient ($R^2 = 0.871$), suggesting that the Elovich model does not provide an adequate fit for Co(II) removal by *P. pavonica* (Figure 8D). However, the parameters α and β of the Elovich model were high, indicating that there are many biosorption sites available for cobalt ion biosorption.

3.7. Adsorption Mechanism

According to FT-IR analysis, the functional groups of the algal biomass containing oxygen improve cobalt biosorption via electrostatic interactions and the formation of hydrogen bonds between the algal surface and Co(II) ions. The peak at 3318 cm^{-1} corresponds to the -OH group found in guluronic acid and mannuronic acid of alginate on the algal biomass surface. Intermolecular hydrogen interactions between cobalt and algal biomass facilitate the biosorption process. Furthermore, the peak shift from 1413 cm^{-1} to 1408 cm^{-1} corresponds to the S=O group, indicating the interaction between fucoidan sulfate groups in algal biomass and Co(II) ions via electrostatic attraction.

The SEM scan also indicated that algal biomass is highly porous with many irregular pores through which biosorption occur.

According to EDX analysis, the disappearance and exchange of some alkali metals during the biosorption process indicated that Co(II) ion biosorption occurred via ion exchange mechanism. Moreover, the presence of cobalt binding energy bands after the biosorption process showed that the algal biomass underwent transformation following cobalt biosorption.

Accordingly, all of these data point to the possibility of Co(II) biosorption onto *P. pavonica* biomass via the formation of hydrogen bonds, electrostatic interaction, and ion exchange mechanisms.

3.8. Biosorption Efficiency of Cobalt Ions from Agricultural Wastewater

The ability of *P. pavonica* to remove Co(II) ions from agricultural wastewater at a cobalt concentration of 40 mg/L was tested. The temperature, pH, total dissolved solids, and electrical conductivity of the effluent were 21.8 °C, 8.92, 751.4 mg/L, and 1174 μS/cm, respectively. Under optimal BBD conditions, the removal efficiency of Co(II) was 85.75%, showing the ability of *P. pavonica* to eliminate Co(II) ions from wastewater.

4. Conclusions

The sustainable use of biomaterials for heavy metal removal from wastewater through biosorption needs information on the most favorable combination of factors to evaluate the performance of the biosorption process in order to maximize the biosorption efficiency of the algae utilized. The response surface methodology is particularly valuable because it decreases the number of experiments needed to determine the optimal circumstances and then conduct experimental validation. BBD calculated the optimal concentration for the

investigated independent parameters to be 5.98 g/L algal inoculum size, 6.73 pH, and an initial Co(II) ion concentration of 21.63 mg/L, and the maximum percentage of Co removal was 84.3%, which agrees with the expected value of 88.55%. The isothermal and kinetic experimental results of cobalt ion biosorption on *P. pavonica* biomass were modeled and well described using Langmuir, Freundlich, and Temkin isotherm models and pseudo-second-order kinetic model. According to the Langmuir model, the maximum biosorption capacity of Co(II) on algal biomass was 17.98 mg/g. *Padina pavonica* is recommended for bioremediation of freshwater and marine sources polluted with Co(II) due to its high Co(II) biosorption efficiency. The internalization of available Co(II) in wastewater allows for quick and simple cobalt removal after the separation of algal biomass by flotation, filtration, sedimentation, etc. The efficacy of *P. pavonica* in large-scale settings such as ponds contaminated with cobalt may vary from our findings and warrant additional research.

Supplementary Materials: The following supporting information can be downloaded at: https://www.mdpi.com/article/10.3390/w16060887/s1, Table S1. The actual response with RSM predicted data (the efficiency of Co(II) removal). Table S2. Comparison of Langmuir biosorption capacity of the studied biosorbent in removing Co(II) ions with different adsorbent capacities. Figure S1. *Padina pavonica*.

Author Contributions: Conceptualization, writing—original draft preparation, investigation, software, methodology, validation, visualization and formal analysis, M.A.F.; writing—review and editing, supervision, validation, formal analysis and visualization, A.S.A.; writing—review and editing and validation, H.M.A.-Y.; investigation, supervision, software, validation, writing—review and editing, and visualization, B.A.R., S.H.A.H. and M.K. All authors have read and agreed to the published version of the manuscript.

Data Availability Statement: Data are contained within the article and Supplementary Materials.

Conflicts of Interest: The authors declare no conflicts of interest.

References

1. Conte, N.; Díez, E.; Almendras, B.; Gómez, J.M.; Rodríguez, A. Sustainable Recovery of Cobalt from Aqueous Solutions Using an Optimized Mesoporous Carbon. *J. Sustain. Metall.* **2023**, *9*, 266–279. [CrossRef]
2. Taha, A.; Hussien, W.; Gouda, S.A. Bioremediation of Heavy Metals in Wastewaters: A Concise Review. *Egypt. J. Aquat. Biol. Fish.* **2023**, *27*, 143–166. [CrossRef]
3. Saleh, T.A.; Tuzen, M.; Sarı, A. Polyethylenimine modified activated carbon as novel magnetic adsorbent for the removal of uranium from aqueous solution. *Chem. Eng. Res. Des.* **2017**, *117*, 218–227. [CrossRef]
4. Akeel, A.; Jahan, A. Role of cobalt in plants: Its stress and alleviation. Contam. *Agric. Sources Impacts Manag.* **2020**, 339–357. [CrossRef]
5. Leyssens, L.; Vinck, B.; Van Der Straeten, C.; Wuyts, F.; Maes, L. Cobalt toxicity in humans—A review of the potential sources and systemic health effects. *Toxicology* **2017**, *387*, 43–56. [CrossRef] [PubMed]
6. Romera, E.; González, F.; Ballester, A.; Blázquez, M.L.; Munoz, J.A. Comparative study of biosorption of heavy metals using different types of algae. *Bioresour. Technol.* **2007**, *98*, 3344–3353. [CrossRef] [PubMed]
7. Finley, B.L.; Monnot, A.D.; Gaffney, S.H.; Paustenbach, D.J. Dose-response relationships for blood cobalt concentrations and health effects: A review of the literature and application of a biokinetic model. *J. Toxicol. Environ. Health-B* **2012**, *15*, 493–523. [CrossRef] [PubMed]
8. Anand, S.R.; Aggarwal, R.; Saini, D.; Sonker, A.K.; Chauhan, N.; Sonkar, S.K. Removal of toxic chromium (VI) from the wastewater under the sunlight-illumination by functionalized carbon nano-rods. *Sol. Energy* **2019**, *193*, 774–781. [CrossRef]
9. Beni, A.A.; Esmaeili, A. Biosorption, an efficient method for removing heavy metals from industrial effluents: A review. *Environ. Technol. Innov.* **2020**, *17*, 100503. [CrossRef]
10. Khoo, K.M.; Ting, Y.P. Biosorption of gold by immobilized fungal biomass. *Biochem. Eng. J.* **2001**, *8*, 51–59. [CrossRef] [PubMed]
11. Ordóñez, J.I.; Cortés, S.; Maluenda, P.; Soto, I. Biosorption of Heavy Metals with Algae: Critical Review of Its Application in Real Effluents. *Sustainability* **2023**, *15*, 5521. [CrossRef]

12. Ordóñez, J.I.; Wong-Pinto, L.; Cortés, S. Biotecnología aplicada a la valorización de relaves mineros. In *Economía Circular en Procesos Mineros*; Cisternas, L., Gálvez, E., Rivas, M., Valderrama, J., Eds.; RIL Editores: Santiago, Chile, 2021; pp. 63–91.

13. Mata, Y.N.; Blázquez, M.L.; Ballester, A.; González, F.; Muñoz, J.A. Characterization of the Biosorption of Cadmium, Lead and Copper with the Brown Alga *Fucus vesiculosus*. *J. Hazard. Mater.* **2008**, *158*, 316–323. [CrossRef]

14. Sheng, P.X.; Ting, Y.P.; Chen, J.P.; Hong, L. Sorption of lead, copper, cadmium, zinc, and nickel by marine algal biomass: Characterization of biosorptive capacity and investigation of mechanisms. *J. Colloid Interface Sci.* **2004**, *275*, 131–141. [CrossRef]

15. Ceban, I.; Lupascu, T.; Mikhalovsky, S.; Nastas, R. Adsorption of Cobalt and Strontium Ions on Plant-Derived Activated Carbons: The Suggested Mechanisms. *C* **2023**, *9*, 71.

16. Guarín, J.R.; Moreno-Pirajan, J.C.; Giraldo, L. Kinetic Study of the Bioadsorption of Methylene Blue on the Surface of the Biomass Obtained from the Algae *D. antarctica*. *J. Chem.* **2018**, *2018*, 2124845. [CrossRef]

17. Fawzy, M.A.; Aloufi, A.S.; Hassan, S.H.; Alessa, A.H.; Alsaigh, A.A.; Koutb, M.; Abdel-Rahim, I.R. Sustainable Use of Marine Macroalga *Sargassum muticum* as a Biosorbent for Hazardous Crystal Violet Dye: Isotherm, Kinetic and Thermodynamic Modeling. *Sustainability* **2023**, *15*, 15064. [CrossRef]

18. Postai, D.L.; Demarchi, C.A.; Zanatta, F.; Melo, D.C.C.; Rodrigues, C.A. Adsorption of rhodamine B and methylene blue dyes using waste of seeds of *Aleurites moluccana*, a low cost adsorbent. *Alex. Eng. J.* **2016**, *55*, 1713–1723. [CrossRef]

19. Salmana, S.M.; Wahaba, M.; Zahoorb, M.; Shahwarc, D.; Sultanaa, S.; Alamzebd, M.; Ahmeda, S. Green mediated biosorption of Pb (II) from aqueous solution using chemically modified low-cost *Grewia optiva* leaves. *Desalin. Water Treat.* **2020**, *195*, 413–420. [CrossRef]

20. Salem, D.M.; Moawad, M.N.; El-Sayed, A.A. Comparative study for bioremediation of cobalt contaminated aqueous solutions by two types of marine macroalgae. *Egypt. J. Aquat. Res.* **2021**, *47*, 13–19. [CrossRef]

21. Elsayed, A.; Moussa, Z.; Alrdahe, S.S.; Alharbi, M.M.; Ghoniem, A.A.; El-Khateeb, A.Y.; Saber, W.I. Optimization of heavy metals biosorption via artificial neural network: A case study of Cobalt (II) sorption by *Pseudomonas alcaliphila* NEWG-2. *Front. Microbiol.* **2022**, *13*, 893603. [CrossRef] [PubMed]

22. Bouras, H.D.; Isik, Z.; Arikan, E.B.; Yeddou, A.R.; Bouras, N.; Chergui, A.; Favier, L.; Amrane, A.; Dizge, N. Biosorption characteristics of methylene blue dye by two fungal biomasses. *Int. J. Environ. Stud.* **2021**, *78*, 365–381. [CrossRef]

23. Arief, V.O.; Trilestari, K.; Sunarso, J.; Indraswati, N.; Ismadji, S. Recent progress on biosorption of heavy metals from liquids using low cost biosorbents: Characterization, biosorption parameters and mechanism studies. *CLEAN–Soil Air Water* **2008**, *36*, 937–962. [CrossRef]

24. Wang, M.; Fu, M.; Li, J.; Niu, Y.; Zhang, Q.; Sun, Q. New insight into polystyrene ion exchange resin for efficient cesium sequestration: The synergistic role of confined zirconium phosphate nanocrystalline. *Chin. Chem. Lett.* **2024**, *35*, 108442. [CrossRef]

25. Sandesh, K.; Suresh Kumar, R.; JagadeeshBabu, P.E. Rapid removal of cobalt (II) from aqueous solution using cuttlefish bones; equilibrium, kinetics, and thermodynamic study. *Asia-Paci. J. Chem. Eng.* **2013**, *8*, 144–153. [CrossRef]

26. Ibrahim, W.M.; Hassan, A.F.; Azab, Y.A. Biosorption of toxic heavy metals from aqueous solution by *Ulva lactuca* activated carbon. *Egypt. J. Basic Appl. Sci.* **2016**, *3*, 241–249. [CrossRef]

27. Omidvar-Hosseini, F.; Moeinpour, F. Removal of Pb (II) from aqueous solutions using *Acacia nilotica* seed shell ash supported $Ni_{0.5}Zn_{0.5}Fe_2O_4$ magnetic nanoparticles. *J. Water Reuse Desal.* **2016**, *6*, 562–573. [CrossRef]

28. Tahoon, M.A.; Siddeeg, S.M.; Salem Alsaiari, N.; Mnif, W.; Ben Rebah, F. Effective heavy metals removal from water using nanomaterials: A review. *Processes* **2020**, *8*, 645. [CrossRef]

29. Ranaweera, K.H.; Godakumbura, P.I.; Perera, B.A. Adsorptive removal of Co (II) in aqueous solutions using clearing nut seed powder. *Heliyon* **2020**, *6*, e03684. [CrossRef] [PubMed]

30. Li, X.; Xiao, Q.; Shao, Q.; Li, X.; Kong, J.; Liu, L.; Zhao, Z.; Li, R. Adsorption of Cd (II) by a novel living and non-living *Cupriavidus necator* GX_5: Optimization, equilibrium and kinetic studies. *BMC Chem.* **2023**, *17*, 54. [CrossRef]

31. Bai, M.T.; Venkateswarlu, P. Fixed bed and batch studies on biosorption of lead using *Sargassum tenerrimum* powder: Characterization, Kinetics and Thermodynamics. *Mater. Today Proc.* **2018**, *5*, 18024–18037.

32. Khalaf, H.A.; El-Sheekh, M.M.; Makhlof, M.E. *Lychaete pellucida* as a novel biosorbent for the biodegradation of hazardous azo dyes. *Environ. Monit. Assess.* **2023**, *195*, 929. [CrossRef]

33. Fawzy, M.A. Biosorption of copper ions from aqueous solution by *Codium vermilara*: Optimization, kinetic, isotherm and thermodynamic studies. *Adv. Powder Technol.* **2020**, *31*, 3724–3735. [CrossRef]

34. Alharbi, N.K.; Al-Zaban, M.I.; Albarakaty, F.M.; Abdelwahab, S.F.; Hassan, S.H.; Fawzy, M.A. Kinetic, isotherm and thermodynamic aspects of Zn^{2+} biosorption by *Spirulina platensis*: Optimization of process variables by response surface methodology. *Life* **2022**, *12*, 585. [CrossRef] [PubMed]

35. Jayan, N.; Bhatlu, M.L.D.; Akbar, S.T. Central composite design for adsorption of Pb (II) and Zn (II) metals on PKM-2 *Moringa oleifera* leaves. *ACS Omega* **2021**, *6*, 25277–25298. [CrossRef] [PubMed]

36. Masoumi, H.; Ghaemi, A.; Gilani, H.G. Synthesis of polystyrene-based hyper-cross-linked polymers for Cd (II) ions removal from aqueous solutions: Experimental and RSM modeling. *J. Hazard. Mater.* **2021**, *416*, 125923. [CrossRef] [PubMed]

37. Ibrahim, A.G.; Baazeem, A.; Al-Zaban, M.I.; Fawzy, M.A.; Hassan, S.H.; Koutb, M. Sustainable Biodiesel Production from a New Oleaginous Fungus, *Aspergillus carneus* Strain OQ275240: Biomass and Lipid Production Optimization Using Box–Behnken Design. *Sustainability* **2023**, *15*, 6836. [CrossRef]

38. Madadgar, S.; Doulati Ardejani, F.; Boroumand, Z.; Sadeghpour, H.; Taherdangkoo, R.; Butscher, C. Biosorption of Aqueous Pb (II), Co (II), Cd (II) and Ni (II) Ions from Sungun Copper Mine Wastewater by *Chrysopogon zizanioides* Root Powder. *Minerals* **2023**, *13*, 106. [CrossRef]

39. Shaban, M.; Abukhadra, M.R.; Khan, A.A.P.; Jibali, B.M. Removal of Congo red, methylene blue and Cr (VI) ions from water using natural serpentine. *J. Taiwan Inst. Chem. Eng.* **2018**, *82*, 102–116. [CrossRef]

40. Martini, S.; Afroze, S.; Roni, K.A. Modified eucalyptus bark as a sorbent for simultaneous removal of COD, oil, and Cr (III) from industrial wastewater. *Alex. Eng. J.* **2020**, *59*, 1637–1648. [CrossRef]

41. Monteiro, C.M.; Castro, P.M.; Xavier Malcata, F. Biosorption of zinc ions from aqueous solution by the microalga *Scenedesmus obliquus*. *Environ. Chem. Lett.* **2011**, *9*, 169–176. [CrossRef]

42. Kumar, P.S.; Kirthika, K. Equilibrium and kinetic study of adsorption of nickel from aqueous solution onto bael tree leaf powder. *J. Eng. Sci. Technol.* **2009**, *4*, 351–363.

43. Pang, J.; Fu, F.; Ding, Z.; Lu, J.; Li, N.; Tang, B. Adsorption behaviors of methylene blue from aqueous solution on mesoporous birnessite. *J. Taiwan Inst. Chem. Eng.* **2017**, *77*, 168–176. [CrossRef]

44. Gao, W.; Zhao, S.; Wu, H.; Deligeer, W.; Asuha, S. Direct acid activation of kaolinite and its effects on the adsorption of methylene blue. *Appl. Clay Sci.* **2016**, *126*, 98–106. [CrossRef]

45. Soleymani, F.; Pahlevanzadeh, H.; Khani, M.H.; Manteghian, M. Biosorption of cobalt (II) by intact and chemically modified brown algae: Optimization using response surface methodology and equilibrium, dynamics and thermodynamics studies. *Iran J. Chem. Eng.* **2014**, *11*, 77.

46. Babu, P.N.; Binnal, P.; Kumar, D.J. Biosorption of Zn^{2+} on non-living biomass of *S. platensis* immobilized on polyurethane foam cubes: Column studies. *J. Biochem. Technol.* **2015**, *6*, 852–859.

47. Yagub, M.T.; Sen, T.K.; Afroze, S.; Ang, H.M. Dye and its removal from aqueous solution by adsorption: A review. *Adv. Colloid Interface Sci.* **2014**, *209*, 172–184. [CrossRef] [PubMed]

48. Danish, M.; Ahmad, T.; Majeed, S.; Ahmad, M.; Ziyang, L.; Pin, Z.; Iqubal, S.S. Use of banana trunk waste as activated carbon in scavenging methylene blue dye: Kinetic, thermodynamic, and isotherm studies. *Bioresour. Technol. Rep.* **2018**, *3*, 127–137. [CrossRef]

49. Esmaili, Z.; Barikbin, B.; Shams, M.; Alidadi, H.; Al-Musawi, T.J.; Bonyadi, Z. Biosorption of metronidazole using *Spirulina platensis* microalgae: Process modeling, kinetic, thermodynamic, and isotherm studies. *Appl. Water Sci.* **2023**, *13*, 63. [CrossRef]

50. Fawzy, M.A.; Alharthi, S. Cellular responses and phenol bioremoval by green alga *Scenedesmus abundans*: Equilibrium, kinetic and thermodynamic studies. *Environ. Technol. Innov.* **2021**, *22*, 101463. [CrossRef]

51. Gonçalves Junior, A.C.; Meneghel, A.P.; Rubio, F.; Strey, L.; Dragunski, D.C.; Coelho, G.F. Applicability of *Moringa oleifera* Lam. pie as an adsorbent for removal of heavy metals from waters. *Rev. Bras. Eng. Agrícola Ambient.* **2013**, *17*, 94–99. [CrossRef]

52. Khani, M.H. Statistical analysis and isotherm study of uranium biosorption by Padina sp. Algae biomass. *Environ. Sci. Pollut. Res.* **2011**, *18*, 790–799. [CrossRef]

53. Fawzy, M.A.; Hifney, A.F.; Adam, M.S.; Al-Badaani, A.A. Biosorption of cobalt and its effect on growth and metabolites of *Synechocystis pevalekii* and *Scenedesmus bernardii*: Isothermal analysis. *Environ. Technol. Innov.* **2020**, *19*, 100953. [CrossRef]

54. Dahiya, S.; Tripathi, R.M.; Hegde, A.G. Biosorption of heavy metals and radionuclide from aqueous solutions by pre-treated arca shell biomass. *J. Hazard. Mater.* **2008**, *150*, 376–386. [CrossRef] [PubMed]

55. Sahu, S.; Pahi, S.; Tripathy, S.; Singh, S.K.; Behera, A.; Sahu, U.K.; Patel, R.K. Adsorption of methylene blue on chemically modified lychee seed biochar: Dynamic, equilibrium, and thermodynamic study. *J. Mol. Liq.* **2020**, *315*, 113743. [CrossRef]

56. Elkhaleefa, A.; Ali, I.H.; Brima, E.I.; Shigidi, I.; Elhag, A.B.; Karama, B. Evaluation of the adsorption efficiency on the removal of lead (II) ions from aqueous solutions using *Azadirachta indica* leaves as an adsorbent. *Processes* **2021**, *9*, 559. [CrossRef]

57. Ashour, M.; Alprol, A.E.; Khedawy, M.; Abualnaja, K.M.; Mansour, A.T. Equilibrium and Kinetic Modeling of Crystal Violet Dye Adsorption by a Marine Diatom, *Skeletonema costatum*. *Materials* **2022**, *15*, 6375. [CrossRef] [PubMed]

58. Al-Zaban, M.I.; Alharbi, N.K.; Albarakaty, F.M.; Alharthi, S.; Hassan, S.H.; Fawzy, M.A. Experimental modeling investigations on the biosorption of methyl violet 2B dye by the brown seaweed *Cystoseira tamariscifolia*. *Sustainability* **2022**, *14*, 5285. [CrossRef]

59. Vijayaraghavan, K.; Jegan, J.; Palanivelu, K.; Velan, M. Biosorption of cobalt (II) and nickel (II) by seaweeds: Batch and column studies. *Sep. Purify. Technol.* **2005**, *44*, 53–59. [CrossRef]

60. Al-Jlil, S.A. Equilibrium study of adsorption of cobalt ions from wastewater using Saudi roasted date pits. *Res. J. Environ. Toxicol.* **2010**, *4*, 1–12. [CrossRef]

61. Hymavathi, D.; Prabhakar, G. Studies on the removal of Cobalt (II) from aqueous solutions by adsorption with *Ficus benghalensis* leaf powder through response surface methodology. *Chem. Eng. Commun.* **2017**, *204*, 1401–1411. [CrossRef]

62. Foroutan, R.; Esmaeili, H.; Abbasi, M.; Rezakazemi, M.; Mesbah, M. Adsorption behavior of Cu (II) and Co (II) using chemically modified marine algae. *Environ. Technol.* **2018**, *39*, 2792–2800. [CrossRef]

63. Esmaeili, A.; Soufi, S.; Rustaiyan, A.; Safaiyan, S.; Mirian, S.; Fallahe, G.; Moazami, N. Biosorption of copper, cobalt and nickel by marine brown alga *Sargassum* sp. in fixed-bed column. *Pak. J. Biol. Sci.* **2007**, *10*, 3919–3922.

64. Cárdenas González, J.F.; Rodríguez Pérez, A.S.; Vargas Morales, J.M.; Martínez Juárez, V.M.; Rodríguez, I.A.; Cuello, C.M.; Fonseca, G.G.; Escalera Chávez, M.E.; Muñoz Morales, A. Bioremoval of cobalt (II) from aqueous solution by three different and resistant fungal biomasses. *Bioinorg. Chem. Appl.* **2019**, *2019*, 8757149. [CrossRef]

65. Rashmi, K.; Sowjanya, T.N.; Mohan, P.M.; Balaji, V.; Venkateswaran, G. Bioremediation of 60Co from simulated spent decontamination solutions. *Sci. Total Environ.* **2004**, *328*, 1–14. [CrossRef]

66. Lupea, M.; Bulgariu, L.; Macoveanu, M. Adsorption of Cobalt (II) from aqueous solution using marine green algae–*Ulva Lactuca* sp. *Bull IP Iasi* **2012**, *58*, 41–47.

67. Uddin, M.K. A review on the adsorption of heavy metals by clay minerals, with special focus on the past decade. *Chem. Eng. J.* **2017**, *308*, 438–462. [CrossRef]

68. Hubbe, M.A.; Azizian, S.; Douven, S. Implications of apparent pseudo-second-order adsorption kinetics onto cellulosic materials: A review. *BioResources* **2019**, *14*, 7582–7626. [CrossRef]

69. Lavado-Meza, C.; De la Cruz-Cerrón, L.; Lavado-Puente, C.; Angeles-Suazo, J.; Dávalos-Prado, J.Z. Efficient Lead Pb (II) Removal with Chemically Modified Nostoc commune Biomass. *Molecules* **2022**, *28*, 268. [CrossRef] [PubMed]

70. Bordoloi, N.; Goswami, R.; Kumar, M.; Kataki, R. Biosorption of Co (II) from aqueous solution using algal biochar: Kinetics and isotherm studies. *Bioresour. Technol.* **2017**, *244*, 1465–1469. [CrossRef]

71. Rangabhashiyam, S.; Anu, N.; Nandagopal Giri, M.S.; Selvaraju, N. Relevance of isotherm models in biosorption of pollutants by agricultural by-products. *J. Environ. Chem. Eng.* **2014**, *2*, 398–414. [CrossRef]

72. Naskar, A.; Majumder, R. Understanding the adsorption behaviour of acid yellow 99 on *Aspergillus niger* biomass. *J. Mol. Liq.* **2017**, *242*, 892–899. [CrossRef]